Vehicle-to-Infrastructure Visible Light Communications: Channel Modelling and Capacity Calculations

Hossien B. Eldeeb, Mohammed Elamassie, and Murat Uysal
Department of Electrical and Electronics Engineering, Özyeğin University, Istanbul, Turkey, 34794.
E-mail: hossien.eldeeb@ozyegin.edu.tr

***Abstract*—In this paper, we investigate the performance of a visible light communication (VLC) system for vehicle-to-infrastructure (V2I) connectivity. Two headlamps of the vehicle serve as wireless transmitters while photodetectors located within the traffic light pole act as wireless receivers. We use non-sequential ray-tracing approach to obtain optical channel impulse responses (CIRs) for the V2I scenario under consideration assuming different positions of the vehicle within the road. Based on the CIRs to model propagation environment as well as the effects of LED non-linear characteristics, we calculate the achievable signal-to-noise ratio and achievable data rates for VLC-based V2I systems.**

***Index Terms*—Vehicular visible light communication, Raytracing, vehicle-to-Infrastructure communication.**

I. Introduction

Intelligent transportation systems (ITSs) aim to improve road safety, traffic flow, and passenger comfort [1] through the use of advanced connectivity, control and sensor technologies. Vehicular connectivity, in various forms such as vehicle-to-vehicle (V2V), vehicle-to-infrastructure (V2I) and infrastructure-to-vehicle (I2V) communications, is considered one of the keys enabling technologies for ITSs. Current deployments typically use radio-based solutions such as LTE-V and DSRC [2]. However, limited radio frequency bands allocated for vehicular networks can suffer high levels of interference in heavy traffic and channel congestion might be particularly problematic for delay-sensitive safety functionalities [3]. Such motivations have prompted researchers to investigate visible light communication (VLC) for vehicular networks [4], [5].

VLC is based on the principle of modulating light-emitting-diode (LED) light at very high speeds beyond the perception of human eyes. This lets the dual use of LED luminaries for both illumination and communication capabilities. VLC is a natural candidate for V2V and V2I/I2V communications since LED-based vehicle headlights and taillights as well as street lights and traffic lights can be employed as VLC transmitters. There is a growing literature on various aspects of vehicular VLC including channel modeling, physical layer design, and multi-user networking, see e.g., [6]–[8].

An important research problem is the development of realistic channel models which will shed lights into fundamental performance limits of vehicular VLC networks [9]. Towards this, there have been some efforts in the literature [4], [10]–[30]. Most of these works focused on V2V channels based on either experimental [4], [10]–[12] or simulation studies [13]–[20]. Some attention was paid on V2I/I2V channels [21]–[30]. A comparison of existing works on V2I/I2V can be found in Table 1. Most of these works build upon some idealistic assumptions which do not reflect the inherent characteristics of vehicular VLC systems. For example, in [21]–[23], [25], [26], ideal Lambertian pattern is used to simulate the vehicle headlamps. This does not match practical headlamps which typically have asymmetrical radiation patterns [4]. In addition, most of these works consider only line-of-sight (LOS) component while reflected rays from the road might have a non-negligible contribution on the level of received power. The impact of road reflectance is discussed in [24], [28], but a fixed reflectance value is assumed for simplicity. This however does not hold for visible light spectrum where wavelength-dependent reflectance should be assumed for a realistic modelling.

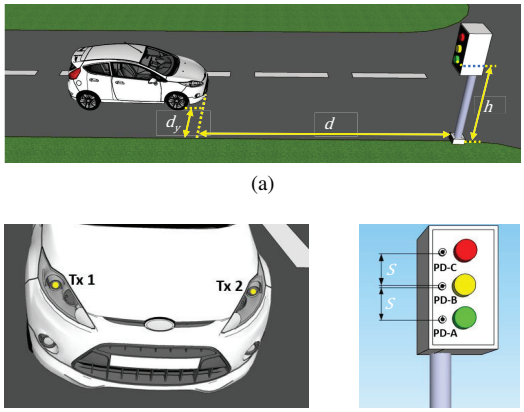

Fig. 1. (a) V2I scenario under consideration and (b) Location of high-beam headlamps (transmitters) and photodetectors (receivers).

In this paper, we aim to address such shortcomings in the current literature and provide a precise channel characterization of VLC-based V2I systems. Specifically, we consider a two-lane road where the vehicle communicates with a traffic light pole. Two headlamps of the vehicle serve as wireless transmitters while three photodetectors located within the traffic light pole adjacent to yellow, red and green LED luminaries to act as wireless receivers. We use non-sequential ray-tracing approach [17], [31]–[33] to obtain optical channel impulse responses (CIRs) for the V2I scenario under consideration assuming different positions of the vehicle within the road. Based on the CIRs to model propagation environment as well as the effects of LED non-linear characteristics, we calculate the achievable signal-to-noise ratio (SNR) and achievable data rates for VLC-based V2I systems. The rest of the paper is organized as follows. In Section II, we present the system

The work of Hossien B. Eldeeb was supported by the European Horizon 2020 MSC ITN (VISION) under Grant 764461. The work of Murat Uysal was supported by the Turkish Scientific and Research Council (TUBITAK) under Grant 215E311.

TABLE I
COMPARISON OF EXISTING WORKS.

System Model	Methodology	Rx	Tx	Observations
[21] I2V scenario using selection combining receiver	Simulation based on spectral model with only LOS.	Photodiode	Red, Green, and Yellow LEDs With Lambertian pattern	In this work, a receiver consisting of two frontends and selection combining circuit is used to improve the SNR values.
[22] I2V in two-lane road	Simulation based on Lambertian model with only LOS & Measurements	Photodiode	Array of WLEDs to fit with standard traffic light	In this study, the channel path loss over the distance is calculated where 42 dB is the attenuation value recorded at 100 m.
[23] I2V scenario using Off-the-shelf LED	Simulation based on Lambertian model with only LOS & Experiment	Photodiode	Commercial-off-the-shelf LED	An analytical model of optical channel path loss between LED traffic light and vehicles is proposed.
[24] I2V in Crossroad and metropolitan	Raytracing using Dialux software assuming fixed reflectance	Photodiode	Street light with Asymmetrical Pattern	This study compared between VL, IR, and UV bands. In which, the UV bands is the worst case in terms of SNR. It is noticed also that I2V link in metropolitan has more dispersive multipath channel behaviour than other cases.
[25] I2V & V2I using Pixel Illumination Model	Simulation based on Lambertian model with only LOS & Measurements	Image sensor	WLED with Lambertian pattern	As an outcome from this study, the channel gain remains constant with the distance if a pixel with maximum luminance is chosen
[26] I2V with Cooperative diversity	Simulation-Lambertian Model with only LOS	Photodiode	WLED with Lambertian pattern	The advantage of using two PDs and Maximal ratio combining (MRC) scheme is investigated.
[27] I2V with MRC	Experiment	Photodiode	RGB LED	The author utilizes MRC scheme and two PDs to increase the transmission distance up to 100 m.
[28] I2V in tunnel	Monte Carlo raytracing assuming fixed reflectance	Photodiode	Commercial street light source	An initial study for I2V channels in the tunnel condition is proposed where insights for the coverage area and the achieved capacity are illustrated.
[29] I2V based on camera as a receiver	Experiment	Camera	Green traffic light	Demonstration for I2V communications based on a green traffic light and a camera receiver is proposed.
[30] I2V based on commercial street light in a two-lane highway road	Raytracing using OpticStudio with wavelength-dependent reflectance	Photodiode	Commercial streetlight with asymmetrical pattern	A simulation study for I2V link based on a commercial streetlight source with asymmetrical radiation pattern. The effect of car velocity and the nearby cars on the received SNR is investigated.

model and describe channel modeling approach. In Section III, we provide capacity analysis. In Section IV, we present simulation results and finally present concluding remarks in Section V.

II. System and Channel Model

As illustrated in Fig. 1.a, we consider a V2I scenario in a two-lane road. We assume that the car moves at the right road lane with a separation distance of d with respect to the traffic light pole. We further define d_y which defines the horizontal shift between the car and the traffic light pole. As illustrated in Fig. 1.b, two high-beam LED headlamps (denoted by Tx 1 and Tx 2) are used as VLC transmitters. These two LEDs are assumed to have an electrical-to-optical conversion of η and a total electrical power budget of P_e. Three photodetectors (PD-A, PD-B, and PD-C) are placed in the traffic light and act as wireless receivers. As illustrated in Fig. 1.b, PD-A is located at a height of h from the ground and a vertical separation of S is assumed between PDs.

For channel modelling, we utilize non-sequential ray-tracing approach which was earlier used for the development of indoor and underwater VLC channel models [31]–[33] and recently applied to V2V VLC [15], [17]. In this method, a 3D simulation platform with CAD models of cars and traffic poles is constructed in OpticStudio® software. Then, we define the coating material of CAD-object surfaces where the scatter fraction and the wavelength-dependent reflectance are specified. The light source specifications such as radiation pattern, optical power, orientations, and the number of emitted rays are then defined. Similarly, receiver specifications such as orientations, field-of-view (FOV) angle, and aperture area are defined. The weather condition is further specified by choosing from different scatter models available in OpticStudio®. Following [34], we utilize Mie scattering model where the radius of the spherical particles, refractive index of particles, and density of particles are provided as inputs to OpticStudio®. After the 3D simulation platform is constructed, non-sequential ray tracing is executed to generate an output file including the power and the path length of each ray that reaches to the receiver. This information is proceed in MATLAB® in order to obtain the CIR. Assume that N_j is the total number of rays reaching the j^{th} PD for a given distance d. Let P_{ij} and τ_{ij} respectively denote the power and the propagation delay of the i^{th} ray, $i = 1, 2, ..., N_j$ received by the j^{th} PD, $j = 1, ..., 3$. The CIR at the j^{th} PD can be expressed as [15], [17]

$$h_j^{\text{opt}}(t) = \sum_{i=1}^{N_j} P_{ij}\, \delta\left(t - \tau_{ij}\right), \tag{1}$$

where δ is the Dirac delta function. The corresponding frequency response is given by $h_j^{\text{opt}}(t) \overset{\text{FT}}{\longleftrightarrow} H_j^{\text{opt}}(f)$. In addition to propagation environment, the LED characteristics might further introduce distortions. Let f_c denote the cut-off frequency of the LED. The LED frequency response is typically given by [35]

$$H^{led}(f) = \frac{1}{1 + j\frac{f}{f_c}}. \tag{2}$$

Therefore, the effective frequency response at the j^{th} PD including the combined effects of both propagation channel and front-end effects is given by $H_j^{\text{eff}}(f) = H_j^{\text{opt}}(f)\, H^{led}(f) \overset{\text{IFFT}}{\longleftrightarrow} h_j^{\text{eff}}(t)$. The path loss can be then computed as

$$PL_j^{\text{eff}} = 10\log_{10}\left(\int_0^{\infty} h_j^{\text{eff}}(t)\, dt\right). \tag{3}$$

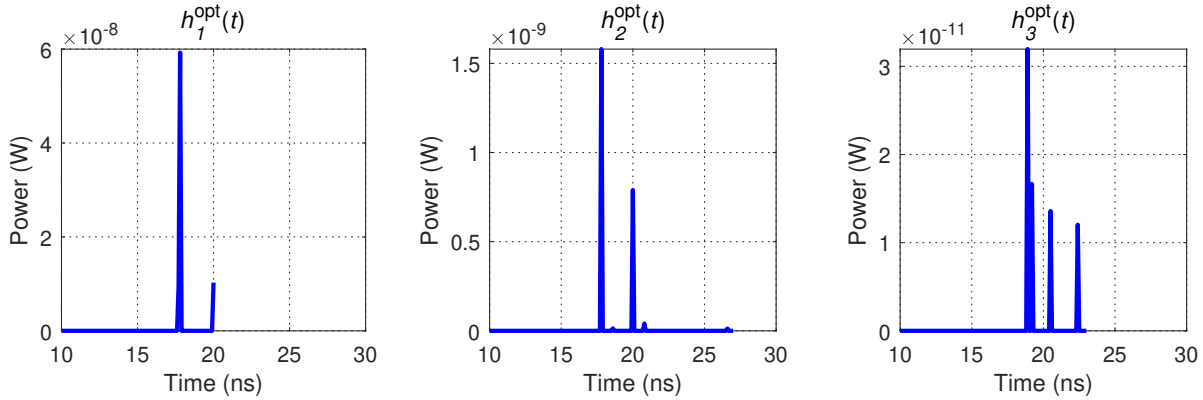

(a)

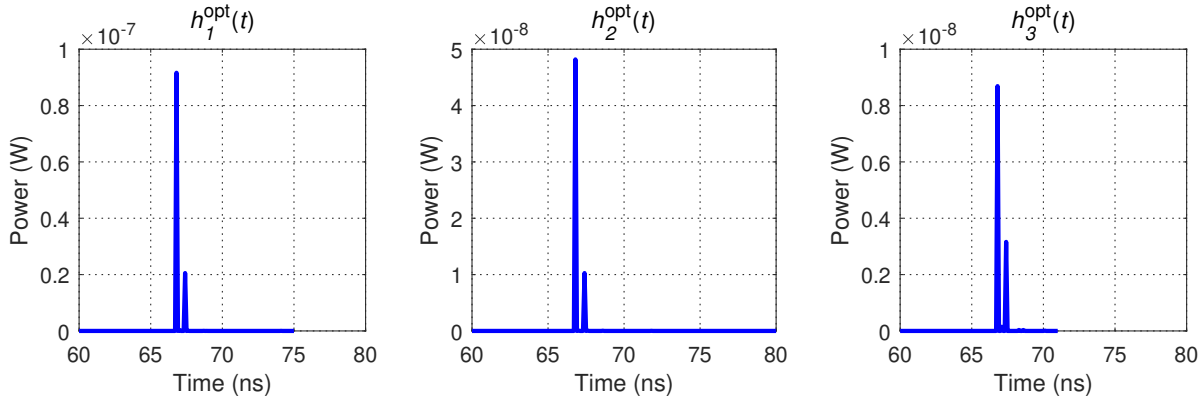

(b)

Fig. 2. Optical CIRs for Scenario II at each PD assuming P_e = 15 dBm (a) d = 5 m (b) d = 20 m

III. Achievable Data Rates

As a performance metric, we consider ergodic capacity which yields the maximum data rate that can be achieved in a communication system. For VLC systems with intensity modulation/direct detection (IM/DD), the transmitted signal is typically constrained in both average and peak values [36]. The exact expression for ergodic capacity is still unknown for IM/DD systems. Consequently, different bounds on the capacity of optical channels are derived in the literature [35], [37]–[39]. For example, it is shown in [39] that the gap between the exact and the lower bound can be neglected for high SNR values and the capacity can be approximated as

$$C \approx \frac{B}{2\ln(2)} \ln\left(1 + \frac{\exp(1)\,\gamma}{2\pi}\right), \tag{4}$$

where γ is the signal-to-noise ratio (SNR) and B is the bandwidth. SNR is given by

$$\gamma = \frac{\left(\eta\, R\, h_{DC}^{\text{eff}}\right)^2 P_{\text{e}}}{\sigma_n^2}, \tag{5}$$

where R is photodetector's responsivity, P_e is electrical transmission power, $h_{DC}^{\text{eff}} = \int_0^\infty h^{\text{eff}}(t)\, dt$ is the DC channel gain. $\sigma_n^2 = N_0 B$ is the noise variance and N_0 is noise power spectral density. Replacing (5) in (4), we have

$$C \approx \frac{B}{2\ln(2)} \ln\left(1 + \frac{\exp(1)\left(\eta R h_{DC}^{\text{eff}}\right)^2 P_{\text{e}}}{2\pi N_0 B}\right). \tag{6}$$

IV. Simulation Results and Discussion

As shown in Fig. 1.a, we consider a V2I scenario in a two-lane road where R2 type road with asphalt coating is considered. The car is modeled as black-colored CAD object with dimensions of Audi A5 Coupe model [40]. The traffic pole is modeled as a CAD object with surface cover of galvanized steel. The values of h and S are assumed to be 2 m and 0.25 m, respectively. In our simulation study, we create the photometric data (i.e., IES file) of the car headlamp under consideration which contains the luminous intensity in all different planes. This photometric file is imported to the OpticStudio® software along with the spectral power distribution of the LED.

We use two Philips Luxeon Rebel white LEDs for car headlamps with P_e = 15 dBm, f_c = 20 MHz, and η = 0.5. We employ photodetectors each with an area of 1 cm^2, FOV angle of 90°, and responsivity of R = 0.28. In simulations, we first obtain CIRs under the assumption of unity transmission optical power. The CIRs can be then scaled for any given value of transmit power. We consider three scenarios:

- **Scenario I:** The car moves at the outer edge of the right lane with a horizontal shift of d_y = 0.25 m from the traffic pole.
- **Scenario II:** The car moves at the middle of the right lane which results in a d_y = 1 m shift with respect to the traffic pole and Scenario.

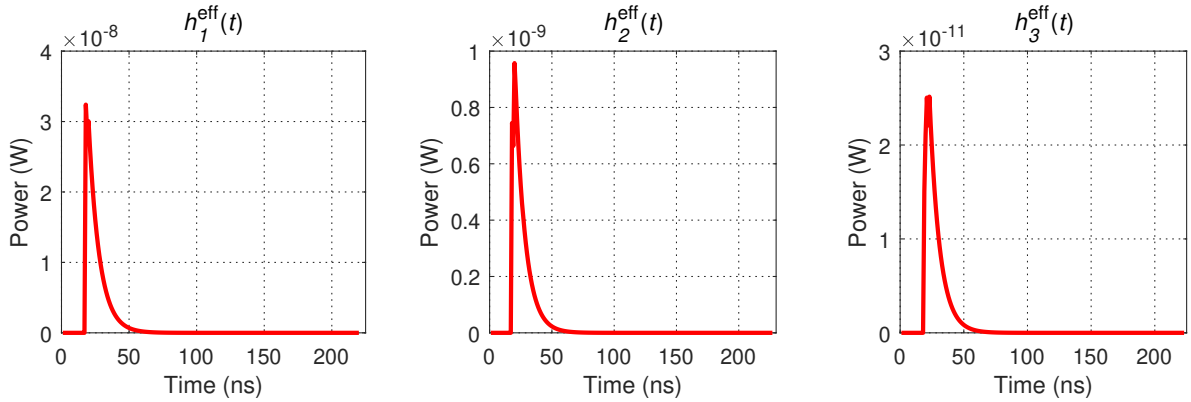

(a)

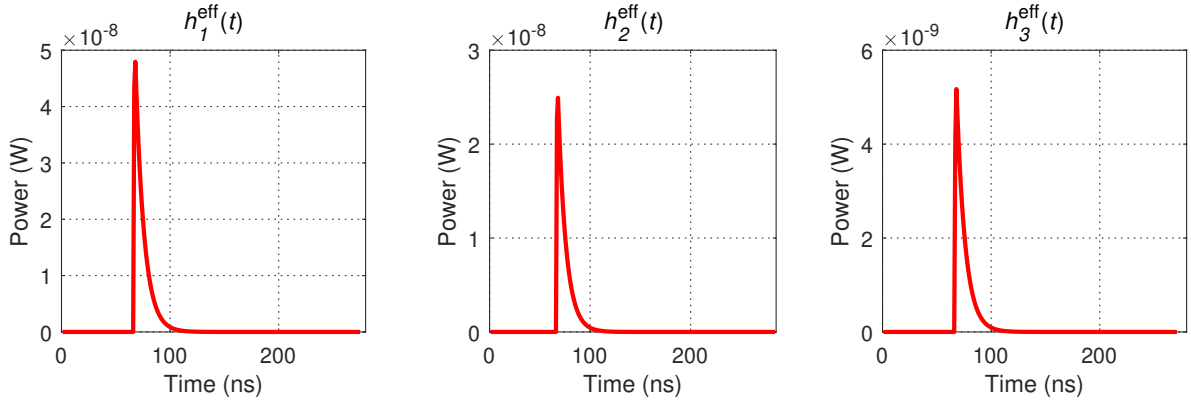

(b)

Fig. 3. Effective CIRs for Scenario II at each PD assuming P_e = 15 dBm and f_c = 20 MHz (a) d = 5 m (b) d = 20 m.

- **Scenario III:** The car moves at the inner edge of the right lane which results in a d_y = 2 m shift with respect to the traffic pole.

In Fig. 2, we provide optical CIRs, i.e., $h_j^{\text{opt}}(t)$, $j = 1, ..., 3$ at distances of d = 5 m and d = 20 m for Scenario II. It can be observed that the CIRs have more than one peak where the highest peak comes from the right headlamp (Tx 1) and the second one comes from the left headlamp (Tx 2). This is due to the fact that signals with different travelling distances will have different arrival times. For example, consider d = 5 m and PD-A (see Fig. 2.a)., the propagation distances from the right and left headlamps to the receiver are given, respectively, as 5.3 m and 6 m. It can be readily confirmed that the peak from the right headlamp occurs at 17.8 ns while the peak from the second headlamp is around 20 ns. It can be also observed that additional peaks are observed due to reflections from road. As seen from Fig. 2.b, as d increases, the distances between two peaks decreases and road reflections disappear.

In Fig. 3, we present the corresponding effective CIRs $h_j^{\text{eff}}(t)$, $j = 1, ..., 3$ for d = 5 m and d = 20 m assuming Scenario II. It is observed that the CIRs broaden in time due to the impact of low-pass nature of LED which dominates the overall characteristics. As a result, the effective CIR turns to be a single peak. It is also observed from Fig. 2 and Fig. 3 that the received power at 20 m is higher than at 5 m. This is due to the impact of receiver height where at shorter distances the receiver can not efficiently see the transmitter.

In Fig. 4, we present the path loss for all scenarios and three PDs under consideration. It is observed that PD-A achieves the highest channel gain while PD-C has the worst gain. This is due to the relatively large difference between its height and the height of car headlamps. For example, consider scenario I and a distance of d = 10 m. The channel gain using PD-A is recorded as PL_1^{eff} = -55.6 dB. This reduces to PL_2^{eff} = -65.8 dB and PL_3^{eff} = -76.9 dB for PD-B and PD-C, respectively. When the lateral shift (d_y) increases, the path loss further increases. For example, consider PD-A and a distance of d = 20 m. The path loss values for scenario I, scenario II, and scenario III are obtained respectively as -59.3 dB, 60.2 dB, and -63.5 dB.

In Fig. 5, the achievable data rates based on (6) are presented. Since the PD-A receives the highest gain with respect to other PDs, it can achieve the highest capacity for all scenarios under consideration. For scenario II and d = 30 m, the maximum data rate that can be supported with PD-A is 54 Mbps. This reduces to 41.8 Mbps and 21.3 Mbps respectively for PD-B and PD-C. It can be also noted that in shorter distances, the lateral shift dominates the overall characteristics. It is also observed that the capacity first increases with the distance until reaching the maximum value because of reducing the horizontal shift, d_y. Then, any increase in the distance results in decreasing of the capacity

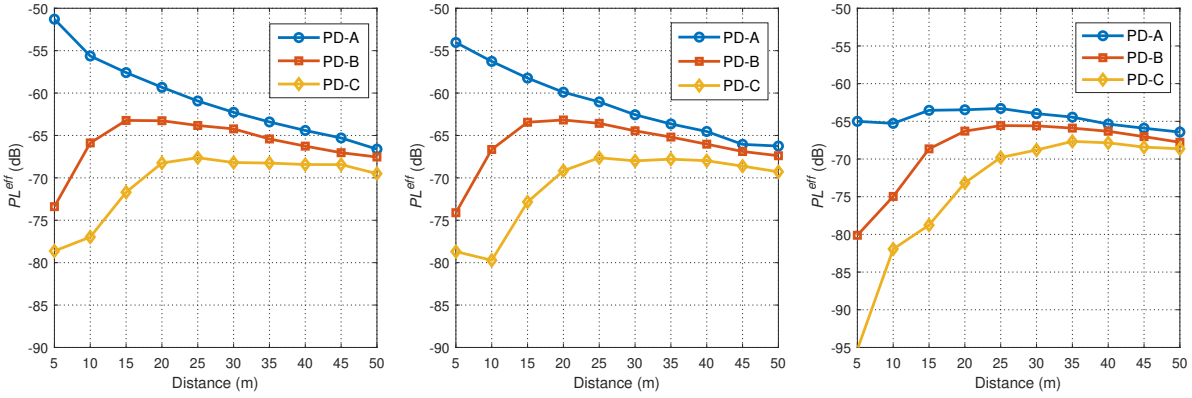

(a) (b) (c)

Fig. 4. Path loss for (a) Scenario I (b) Scenario II (c) Scenario III for transmit power of P_e = 15 dBm and front-end bandwidth of 20 MHz.

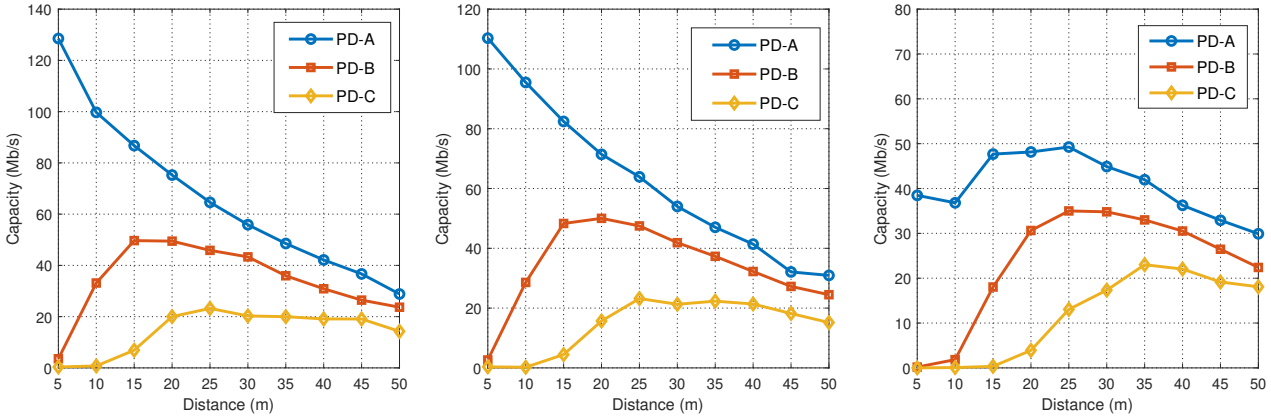

(a) (b) (c)

Fig. 5. Achievable data rate versus distance at each PD for (a) Scenario I (b) Scenario II (c) Scenario III for transmit power of P_e = 15 dBm and front-end bandwidth of 20 MHz.

due to the effect of longitudinal distance, d.

So far, we assumed the employment of single photodetector. It is possible to take advantage of all three photodetectors. For this purpose, we employ equal gain combining (EGC) in Fig. 6. EGC uses a direct sum of the branch signals from all photodetectors with equal weighting to all branches, which result in increasing of overall received SNR. As observed from Fig. 6, the achievable data rate significantly increases due to such combining.

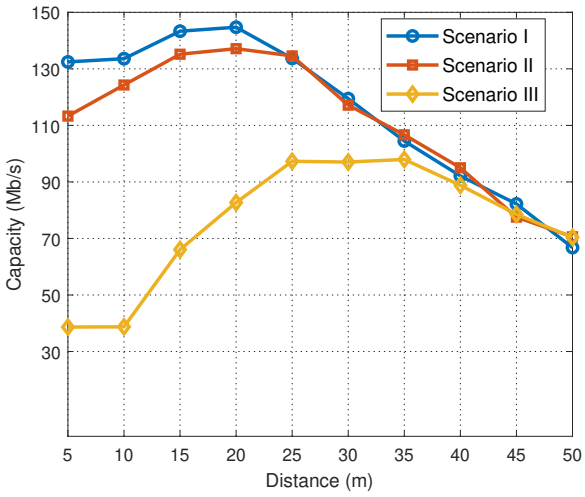

Fig. 6. Achievable data rate versus distance for three photodetectors deployment case (equal gain combining).

V. Conclusion

In this paper, we have investigated the channel characteristics of V2I VLC link in a two-lane road. The two headlamps of the vehicle are utilized as wireless transmitters to communicate with the traffic pole which has three photodetectors located adjacent to yellow, red, and green LED luminaries. Non-sequential ray tracing has been adopted to obtain realistic CIRs. In addition to the impact of optical CIRs, the LED front-end has been also shown to strongly affect the channel. By assuming different locations of the vehicle within the road, the effect of lateral shift between the vehicle and the infrastructure has been investigated. By taking into account all of these parameters, we have calculated the achievable data rates of all V2I scenarios under consideration.

REFERENCES

[1] A.Perallos, U. Hernandez-Jayo, I. J. G. Zuazola, and E. Onieva, *Intelligent Transport Systems: Technologies and Applications*. JohnWiley & Sons, 2015.

[2] R. Molina-Masegosa and J. Gozalvez, "LTE-V for sidelink 5G V2X vehicular communications: A new 5G technology for short-range vehicle-to-everything communications," *IEEE Veh. Technol. Mag.*, vol. 12, no. 4, pp. 30–39, 2017.

[3] L. U. Khan, "Visible light communication: Applications, architecture, standardization and research challenges," *Digit. Commun. Netw.*, vol. 3, no. 2, pp. 78–88, 2017.

[4] M. Uysal, Z. Ghassemlooy, A. Bekkali, A. Kadri, and H. Menouar, "Visible light communication for vehicular networking: performance study of a V2V system using a measured headlamp beam pattern model," *IEEE Veh. Technol. Mag.*, vol. 10, no. 4, pp. 45–53, 2015.

[5] T. Yamazato, I. Takai, H. Okada, T. Fujii, T. Yendo, S. Arai, M. Andoh, T. Harada, K. Yasutomi, K. Kagawa *et al.*, "Image-sensor-based visible light communication for automotive applications," *IEEE Commun. Mag.*, vol. 52, no. 7, pp. 88–97, 2014.

[6] P. H. Pathak, X. Feng, P. Hu, and P. Mohapatra, "Visible light communication, networking, and sensing: A survey, potential and challenges," *IEEE Commun. Surveys Tuts.*, vol. 17, no. 4, pp. 2047–2077, 2015.

[7] A.-M. Cailean and M. Dimian, "Impact of ieee 802.15. 7 standard on visible light communications usage in automotive applications," *IEEE Commun. Mag.*, 2017.

[8] B. Aly, M. Elamassie, B. Kebapci, and M. Uysal, "Experimental evaluation of a software defined visible light communication system," in *IEEE ICC 2020 Workshop on Optical Wireless Communications (IEEE ICC'20 Workshop - OWC)*, Dublin, Ireland, Jun. 2020.

[9] A.-M. Căilean and M. Dimian, "Current challenges for visible light communications usage in vehicle applications: A survey," *IEEE Commun. Surveys Tuts.*, vol. 19, no. 4, pp. 2681–2703, 2017.

[10] W. Viriyasitavat, S.-H. Yu, and H.-M. Tsai, "Short paper: Channel model for visible light communications using off-the-shelf scooter taillight," in *IEEE Vehicular Networking Conference*. IEEE, 2013, pp. 170–173.

[11] Y. H. Kim, W. A. Cahyadi, and Y. H. Chung, "Experimental demonstration of vlc-based vehicle-to-vehicle communications under fog conditions," *IEEE Photon. J*, vol. 7, no. 6, pp. 1–9, 2015.

[12] B. Turan, G. Gurbilek, A. Uyrus, and S. C. Ergen, "Vehicular VLC frequency domain channel sounding and characterization," in *IEEE Vehicular Networking Conference (VNC)*. IEEE, 2018, pp. 1–8.

[13] S. Lee, J. K. Kwon, S.-Y. Jung, and Y.-H. Kwon, "Evaluation of visible light communication channel delay profiles for automotive applications," *EURASIP j. Wireless Commun. Netw.*, vol. 2012, no. 1, p. 370, 2012.

[14] P. Luo, Z. Ghassemlooy, H. Le Minh, E. Bentley, A. Burton, and X. Tang, "Performance analysis of a car-to-car visible light communication system," *Applied Optics*, vol. 54, no. 7, pp. 1696–1706, 2015.

[15] M. Elamassie, M. Karbalayghareh, F. Miramirkhani, R. C. Kizilirmak, and M. Uysal, "Effect of fog and rain on the performance of vehicular visible light communications," in *IEEE 87th Vehicular Technology Conference (VTC Spring)*. IEEE, 2018, pp. 1–6.

[16] A. Al-Kinani, J. Sun, C.-X. Wang, W. Zhang, X. Ge, and H. Haas, "A 2-D non-stationary GBSM for vehicular visible light communication channels," *IEEE Trans. Wireless Commun.*, vol. 17, no. 12, pp. 7981–7992, 2018.

[17] H. B. Eldeeb, F. Miramirkhani, and M. Uysal, "A path loss model for vehicle-to-vehicle visible light communications," in *15th International Conference on Telecommunications (ConTEL)*. IEEE, 2019, pp. 1–5.

[18] Z. Cui, P. Yue, X. Yi, and J. Li, "Research on non-uniform dynamic vehicle-mounted VLC with receiver spatial and angular diversity," in *IEEE International Conference on Communications (ICC)*. IEEE, 2019, pp. 1–7.

[19] H. B. Eldeeb and M. Uysal, "Vehicle-to-vehicle visible light communication: How to select receiver locations for optimal performance?" in *11th International Conference on Electrical and Electronics Engineering (ELECO)*. IEEE, 2019, pp. 402–405.

[20] M. Karbalayghareh, F. Miramirkhani, H. B. Eldeeb, R. C. Kizilirmak, S. M. Sait, and M. Uysal, "Channel modelling and performance limits of vehicular visible light communication systems," *IEEE Trans. Veh. Technol.*, pp. 1–1, 2020.

[21] I. E. Lee, M. L. Sim, and F. W.-L. Kung, "Performance enhancement of outdoor visible-light communication system using selective combining receiver," *IET optoelectronics*, vol. 3, no. 1, pp. 30–39, 2009.

[22] N. Kumar, D. Terra, N. Lourenco, L. N. Alves, and R. L. Aguiar, "Visible light communication for intelligent transportation in road safety applications," in *7th International Wireless Communications and Mobile Computing Conference*. IEEE, 2011, pp. 1513–1518.

[23] K. Cui, G. Chen, Z. Xu, and R. D. Roberts, "Traffic light to vehicle visible light communication channel characterization," *Applied optics*, vol. 51, no. 27, pp. 6594–6605, 2012.

[24] J.-H. Lee and S.-Y. Jung, "SNR analyses of the multi-spectral light channels for optical wireless LED communications in intelligent transportation system," in *IEEE 79th Vehicular Technology Conference (VTC Spring)*. IEEE, 2014, pp. 1–5.

[25] T. Yamazato, M. Kinoshita, S. Arai, E. Souke, T. Yendo, T. Fujii, K. Kamakura, and H. Okada, "Vehicle motion and pixel illumination modeling for image sensor based visible light communication," *IEEE J. Sel. Areas Commun.*, vol. 33, no. 9, pp. 1793–1805, 2015.

[26] Z. Cui, P. Yue, and Y. Ji, "Study of cooperative diversity scheme based on visible light communication in vanets," in *International Conference on Computer, Information and Telecommunication Systems (CITS)*. IEEE, 2016, pp. 1–5.

[27] Y. Wang, X. Huang, J. Shi, Y.-q. Wang, and N. Chi, "Long-range high-speed visible light communication system over 100-m outdoor transmission utilizing receiver diversity technology," *Opt. Eng.*, vol. 55, no. 5, p. 056104, 2016.

[28] E. Torres-Zapata, V. Guerra, J. Rabadan, R. Perez-Jimenez, and J. M. Luna-Rivera, "Vehicular communications in tunnels using VLC," in *15th International Conference on Telecommunications (ConTEL)*. IEEE, 2019, pp. 1–6.

[29] E. Eso, Z. Ghassemlooy, S. Zvanovec, A. Gholami, A. Burton, N. B. Hassan, and O. I. Younus, "Experimental demonstration of vehicle to road side infrastructure visible light communications," in *2019 2nd West Asian Colloquium on Optical Wireless Communications (WACOWC)*. IEEE, 2019, pp. 85–89.

[30] M. S. Demir, H. B. Eldeeb, and M. Uysal, "Comp-based dynamic handover for vehicular vlc networks," *IEEE Commun. Lett.*, 2020.

[31] F. Miramirkhani and M. Uysal, "Channel modeling and characterization for visible light communications," *IEEE Photon. J*, vol. 7, no. 6, pp. 1–16, 2015.

[32] M. Elamassie, F. Miramirkhani, and M. Uysal, "Channel modeling and performance characterization of underwater visible light communications," in *2018 IEEE International Conference on Communications Workshops (ICC Workshops)*, 2018, pp. 1–5.

[33] M. Elamassie, F. Miramirkhani, and M. Uysal, "Performance characterization of underwater visible light communication," *IEEE Trans. Commun.*, vol. 67, no. 1, pp. 543–552, 2018.

[34] M. Uysal, C. Capsoni, Z. Ghassemlooy, A. Boucouvalas, and E. Udvary, *Optical wireless communications: an emerging technology*. Springer, 2016.

[35] L. Grobe and K.-D. Langer, "Block-based pam with frequency domain equalization in visible light communications," in *IEEE Globecom Workshops (GC Wkshps)*. IEEE, 2013, pp. 1070–1075.

[36] A. Lapidoth, S. M. Moser, and M. A. Wigger, "On the capacity of free-space optical intensity channels," *IEEE Trans. Inf. Theory*, vol. 55, no. 10, pp. 4449–4461, 2009.

[37] J.-B. Wang, Q.-S. Hu, J. Wang, M. Chen, and J.-Y. Wang, "Tight bounds on channel capacity for dimmable visible light communications," *J. Lightw. Technol.*, vol. 31, no. 23, pp. 3771–3779, 2013.

[38] A. Chaaban, J.-M. Morvan, and M.-S. Alouini, "Free-space optical communications: Capacity bounds, approximations, and a new sphere-packing perspective," *IEEE Trans. Commun.*, vol. 64, no. 3, pp. 1176–1191, 2016.

[39] L. Yin and H. Haas, "Physical-layer security in multiuser visible light communication networks," *IEEE J. Sel. Areas Commun.*, vol. 36, no. 1, pp. 162–174, 2017.

[40] Audi A5., https://www.audiusa.com/models/audi-a5-coupe, [Accessed: May 26, 2020].